Inorganic Chemistry

ARTICLE

pubs.acs.org/IC

Unprecedented Lanthanide-Containing Coordination Polymers Constructed from Hexanuclear Molecular Building Blocks: $\{[Ln_6O(OH)_8](NO_3)_2(bdc)(Hbdc)_2\cdot 2NO_3\cdot H_2bdc\}_\infty$

Guillaume Calvez,[†,‡] Carole Daiguebonne,[†,‡] and Olivier Guillou*[,†,‡]

[†]Université européenne de Bretagne, France

[‡]INSA, UMR 6226 "Sciences Chimiques de Rennes", F-35708 Rennes, France

Supporting Information

ABSTRACT: Reactions in acetonitrile between 1,4-benzene-dicarboxylic acid ($C_8H_6O_4$) and a hexanuclear complex of lanthanide $[Ln_6O(OH)_8(NO_3)_6\cdot 2NO_3]$ with Ln = Y or Tb lead to 1D-coordination polymers with the general chemical formula $\{[Ln_6O(OH)_8](NO_3)_2(bdc)(Hbdc)_2\cdot 2NO_3\cdot H_2bdc\}_\infty$ where H_2bdc stands for 1,4-benzene-dicarboxylic acid (or terephthalic acid). These two compounds are isostructural. The crystal structure has been solved on the basis of the X-ray powder diffraction diagram of the Y-containing compound. This compound crystallizes in the triclinic system, space group $P\bar{1}$ (no. 2) with a = 10.4956(6) Å, b = 11.529(2) Å, c = 12.357(2) Å, α = 86.869(9)°, β = 114.272(6)°, γ = 71.624(7)°, V = 1264.02 Å^3, and Z = 2. The crystal structure can be described as the juxtaposition of linear chains of hexanuclear entities linked to each other by terephthalate ligands. Two additional partially protonated terephthalate ligands spreading laterally to the chain are bound to each hexanuclear entity. Another diprotonated terephthalic ligand and two nitrate ions ensuring the electroneutrality of the crystal structure lie in the interchain space. These two compounds are thermally stable until 200 °C. Thanks to a so-called antenna effect, the Tb-containing compound, despite short intermetallic distances, exhibits a strong luminescence under UV irradiation.

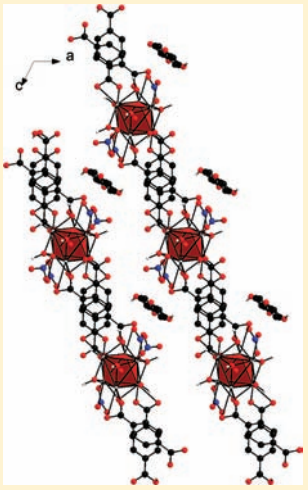

INTRODUCTION

For almost a decade, there has been a great deal of activity devoted to lanthanide-containing coordination polymers.[1] This activity is motivated by their ability to provide potentially porous materials[2−6] and by their interesting luminescent properties.[7−10] Most of the reported works devoted to lanthanide-containing coordination polymers focus on the choice of the ligand.[11,12] Actually, although the validity of the approach has been demonstrated for transition metal ions,[13,14] there are only a few examples of lanthanide-containing coordination polymers in which polynuclear complexes act as metallic centers.[15−25] Moreover, all of these compounds have been obtained using simple lanthanide ion salts as starting materials in one-pot syntheses. These synthetic strategies do not allow easy control of the molecular framework design because the polynuclear entities are not pre-existing and form during the coordination polymer construction. This difficulty arises because, while the cluster chemistry of d-block transition metals is now firmly established,[26,27] the analogous chemistry involving the lanthanide ions is rather underdeveloped. Actually, to date, only a few polynuclear lanthanide complexes have been reported. Most of them, ranging from dinuclear to pentadecanuclear complexes,[16,28−37] have been obtained by the use of ancillary ligands that allow the control of the hydrolysis. Unfortunately, these entities are very unstable in solution[29] and cannot be used as molecular precursors for further chemistry.

A second synthetic route, first described 15 years ago,[38−45] leads to hexanuclear lanthanide complexes with general chemical formula $[Ln_6O(OH)_8(NO_3)_6(H_2O)_{12}]^{2+}$ with Ln = Sm−Yb. This route consists of using lanthanide nitrate as a starting material and in hydrolyzing it by the addition of sodium hydroxide. This synthetic pathway is based on a subtle balance between the various experimental parameters (pH, concentrations, temperature, etc.). The main difficulty encountered during the syntheses of these complexes is to avoid the formation of very stable polymeric species such as $Ln(OH)_2NO_3$,[27,39,40] $LnONO_3$,[46] and $Ln(OH)_3$.[47]

Thanks to this synthetic method, numerous polymorphic phases of such hexanuclear lanthanide complexes with the general chemical formula $[Ln_6O(OH)_8(NO_3)_6(H_2O)_n]\cdot 2NO_3\cdot mH_2O$, with $0 \le m \le 6$, $0 \le n \le 14$, and Ln = Ce−Lu or Y, have been reported so far.[24,25,42,43,45,48,49] All of these compounds have been structurally characterized. All of the crystal structures are very similar. They can be described as the juxtaposition of perfect octahedrons with one lanthanide ion in each vertex and one μ_6-O^{2-} anion at the center. Each face of the octahedrons is shaped by

Received: October 7, 2010
Published: March 07, 2011

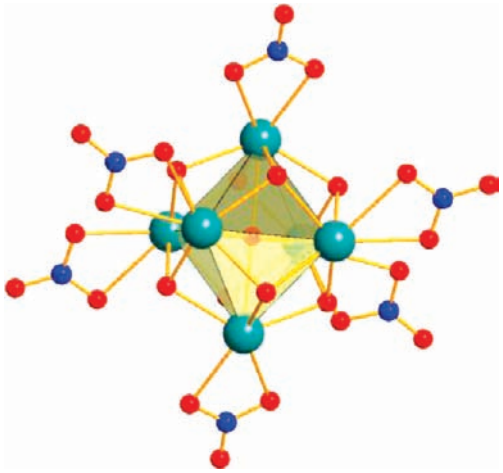

Figure 1. Hexanuclear dicationic core $[Ln_6O(OH)_8(NO_3)_6]^{2+}$ common to all polymorphic phases.

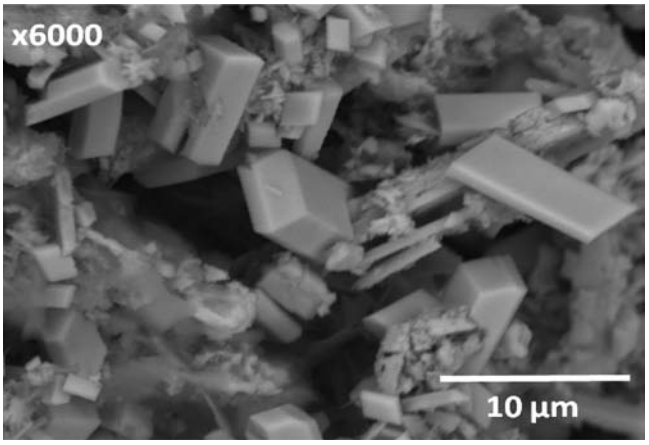

Figure 2. SEM observation of a microcrystalline powder of $\{[Y_6O(OH)_8](NO_3)_2(bdc)(Hbdc)_2\cdot 2NO_3\cdot H_2bdc\}_\infty$.

a μ_3-OH^- anion, and a nitrate ion is bound to each lanthanide ion in a bidentate manner (Figure 1).

The use of hydrated hexanuclear complexes as molecular precursors has always provoked the decomposition of the hexanuclear entities. Actually, because of their high hydration rate, the hydrated complexes slowly hydrolyze during the reaction even in dry organic solvent.[50,51] Therefore, we have decided to use the anhydrous phase[25] as a starting material. We want to report here the synthesis and the crystal structure of the first lanthanide-containing coordination polymer obtained by using a pre-existing hexanuclear complex as a starting building block.

EXPERIMENTAL SECTION

Synthesis of the Microcrystalline Powder of $\{[Ln_6O(OH)_8](NO_3)_2(bdc)(Hbdc)_2\cdot 2NO_3\cdot H_2bdc\}_\infty$ with Ln = Y or Tb. Benzene-1,4-dicarboxylic acid (H_2bdc) was purchased from Acros Organics and used without further purification. Anhydrous acetonitrile was purchased from Acros Organics and kept on molecular sieves. Hydrated lanthanide nitrates were purchased from STREM Chemicals and used without any further purification. Then, the anhydrous hexanuclear complexes were synthesized according to procedures that have already been described elsewhere.[25,49]

Table 1. Chemical Analyses Results for $\{[Ln_6O(OH)_8](NO_3)_2(bdc)(Hbdc)_2,2NO_3,H_2bdc\}_\infty$ with Ln = Y or Tb

		anal. calculated (found)				
Ln	MW (g mol^{-1})	Ln (%)	O (%)	N (%)	C (%)	H (%)
Y	1594.0	33.5 (31.4)	37.1 (41.1)	3.5 (3.5)	24.1 (21.9)	1.8 (2.1)
Tb	2014.1	47.3 (45.0)	29.4 (32.5)	2.8 (2.8)	19.1 (18.1)	1.4 (1.6)

A total of 0.05 mmol of $[Ln_6(\mu_6\text{-}O)(\mu_3\text{-}OH)_8(NO_3)_8]_\infty$ (with Ln = Y or Tb), 0.25 mmol of $bdcH_2$, and 3 mL of dry acetonitrile have been put in a 24 mL Parr autoclave. The mixtures have been heated at 130 °C for 50 h and then allowed to slowly cool down at a cooling rate of 1 °C per hour. The resulting solids have been filtered off and dried under Ar. The yields of the syntheses are roughly 90% (regarding the initial amount of hexanuclear complex). The monophasic character of the microcrystalline powders has been checked by SEM observations (see Figure 2). These observations reveal that the powders are constituted by two phases. The more abundant one is made of well shaped prismatic microcrystals (length ≈ 1−10 μm), while the less abundant one (probably terephthalic acid impurity) is made of very small crystals. This impurity is almost impossible to wash without destroying the interesting phase, and trying to use less of this reagent produced significantly less crystalline powder. The relative weight of this impurity is very low, as demonstrated by the results of the elemental analysis (Table 1).

The IR spectra, measured on KBr pellets, clearly show the characteristic bands of both protonated and deprotonated carboxylate groups, that is, 1410 cm^{-1} and 1380 cm^{-1} for −COOH and $-COO^-$, respectively. The characteristic band of nitrate at 1340 cm^{-1} is also observed. On the other hand, the spectrum does not show any characteristic band for either a water molecule or nitrile functions.

The TGA measurements confirm that there is no solvent departure. They also confirm the molecular weight of the compounds.

The isostructurality of the two compounds has been assumed on the basis of their XRD diagrams.

X-Ray Powder Diffraction. The X-ray powder diffraction diagrams have been collected using a Panalytical X'Pert Pro diffractometer with an X'celerator detector. The recording conditions were 40 kV and 40 mA for Cu Kα (λ = 1.542 Å); the diagrams were recorded in the θ/θ mode over 11 h between 5° and 75° (8378 measurements) with a step size of 0.0084° in 2θ and a scan time of 600 s.

X-Ray Structure Determination of Compound $\{[Y_6O(OH)_8](NO_3)_2(bdc)(Hbdc)_2\cdot 2NO_3\cdot H_2bdc\}_\infty$. To solve the structure of the Y-containing compound, we have used the modeling and simulation software Materials Studio Modeling.[52] This software is convenient for molecular materials because it is able to compute a simulated annealing on fixed groups of atoms, here, for example, the octahedral hexanuclear complex and the ligand molecules.

First, we have calculated cell parameters convenient with the diffraction diagram. Due to the presence of small amounts of terephthalic acid in the final powder, we have ignored three peak positions (17.45°, 25.23°, 27.88°). These peaks correspond to the three main peaks of terephthalic acid (ICDD number 31-1916). To obtain the cell parameters of our new compound, we have used the Dicvol algorithm included in the "Powder Indexing" module of MS Modeling. The 15 more intense peaks match with a triclinic cell with a Smith and Snyder figure of merit[53] F_{15} = 16.7 (0.0082, 109). The obtained cell parameters were close to the ones finally reported but were not yet refined. The volume of the unit cell was about 1200 Å^3. Therefore, it has been possible to make a hypothesis on the content of the cell.

On the basis of elemental analysis, thermal analysis, and IR spectra, we have made the hypothesis of one hexanuclear complex per four nitrate

dx.doi.org/10.1021/ic102036q |*Inorg. Chem.* 2011, 50, 2851–2858

ions and four terephthalate ligands. This hypothesis implies 79 no-H atoms in the formula motif; one such motif per unit cell leads to a value of 15.2 Å^3 per no-H atom, which is similar to what has been previously observed in other yttrium-based hexanuclear phases (15.4 Å^3 per no-H atoms in $[Y_6O(OH)_8(NO_3)_6(H_2O)_{12}]\cdot 2NO_3\cdot 4H_2O$ for example[42]).

With the help of MS Modeling software, we have filled the unit cell with these nine motion groups, each possessing six degrees of freedom. At this stage, no less than 54 DOFs were necessary for describing the unit cell. A few preliminary tests with Rietveld refinement have shown that the central oxygen of the hexanuclear octahedral complex was actually positioned on an inversion center, so the corresponding motion group lost its three translational degrees of freedom, conserving only its three rotational DOFs. Due to this probable inversion center, the eight other independent groups transformed into only four independent groups with six DOFs, so the total number of DOFs decreased significantly to 27.

After thousands of configurations were checked, the software proposed a chemically suitable molecular structure that we refined using Rietveld calculations with a global isotropic temperature factor.[54] Crystal and final structure refinement data are listed in Table 2. The experimental and calculated diffraction diagrams are shown in Figure 3. Full details of the X-ray structure of the yttrium-containing compound have been deposited with the Cambridge Crystallographic Data Center under the depository number CCDC-784583 and can be obtained, on request, upon mentioning the authors and a reference to the present publication. Selected bond distances and angles are listed respectively in Tables 3 and 4.

Thermal Analysis. Thermogravimetric and thermal differential analyses were performed in a platinum crucible under a nitrogen atmosphere between room temperature and 1000 °C with a heating rate of 5 °C min^{-1} using a Perkin-Elmer Pyris-Diamond thermal analyzer.

Thermal dependence X-ray diffraction experiments have been performed using a Panalytical X'Pert Pro diffractometer with an X'celerator detector using Cu Kα_1 radiation in the range 5−75° in 2θ. The heating of the samples (from room temperature to 1000 °C) was performed using an Anton Paar HTK 1200 furnace under a nitrogen atmosphere.

Solid State Luminescence Measurements. Solid state emission spectra were measured on a Perkin-Elmer LS-55 fluorescence spectrometer with a pulse Xe lamp. The slit width was 2.5 nm for excitation and 2.5 nm for emission.

Luminescence spectra were all recorded at room temperature between 200 and 800 nm under identical operating conditions without turning the lamp off to ensure a valid comparison between the emission spectra. Reproducibility of the measurements has been carefully checked by reproducing them several times. The data were collected at 100 nm min^{-1} in phosphorescence mode with a 0.05 ms delay time between the excitation pulse and the emission measurement. The quantum yield measurements performed on a Horiba Jobin-Yvon Fluorolog 3 showed a rather high value of (Ec − Ea/La − Lc) around 59% (Ec, emission spectrum of the sample; Ea, "blank" emission spectrum; La, "blank" absorption; and Lc, sample absorption around excitation wavelength).

Colorimetric Measurements. The CIE (Commission Internationale de l'Eclairage) (*x*,*y*) emission color coordinates[55] were obtained using a MSU-003 colorimeter (Majantys) with the PhotonProbe 1.6.0 Software (Majantys). [Color measurements: 2°, CIE 1931, step 5 nm, under 312 nm UV light $X = k \times \int_{390nm}^{790nm} I_\lambda \times x_\lambda$, $Y = k \times \int_{390nm}^{790nm} I_\lambda \times y_\lambda$, $Z = k \times \int_{390nm}^{790nm} I_\lambda \times z_\lambda$, with k constant for the measurement system I_λ, sample spectrum intensity (wavelength depending), x_λ, y_λ, and z_λ trichromatic values $x = X/X + Y + Z$, $y = Y/X + Y + Z$, $z = Z/X + Y + Z$. Mean *xyz* values are given for each sample, which act as light sources (luminescent samples). Standards from Phosphor Technology used, calibrated at 312 nm: Gd_2O_2S:Eu, Gd_2O_2S:Tb]. The excitation wavenumber was 312 nm. As a reference, the emission color coordinates of the standard red phosphor Gd_2O_2S:Eu (x = 0.667, y = 0.330) and green phosphor Gd_2O_2S:Tb (x = 0.328, y = 0.537) from Phosphor Technology were measured.

Table 2. Experimental Data for the X-Ray Diffraction Study of $\{[Y_6O(OH)_8](NO_3)_2(bdc)(Hbdc)_2, 2NO_3, H_2bdc\}_\infty$

molecular formula	$C_{32}\ O_{37}\ Y_6\ N_4\ H_{28}$
fw	1594.01
temperature (K)	293
cryst syst	triclinic
space group	$P\bar{1}$ (no. 2)
a (Å)	10.4956(6)
b (Å)	11.529(2)
c (Å)	12.357(2)
α (deg)	86.869(9)
β (deg)	114.272(6)
γ (deg)	71.624(7)
V (Å^3)	1264.02
Z	2
λ (Å)	1.5418
ρ_{calcd} (g cm^{-3})	2.094
pattern range (2θ deg)	5−45
step size (2θ deg)	0.0084
step scan time (s)	600
no. contributing reflns (Kα_1 + Kα_2)	323
no. refinement params	27 structural params refined (27 DOF)
	6 profile params refined
Rwp	0.0608
Rp	0.0427

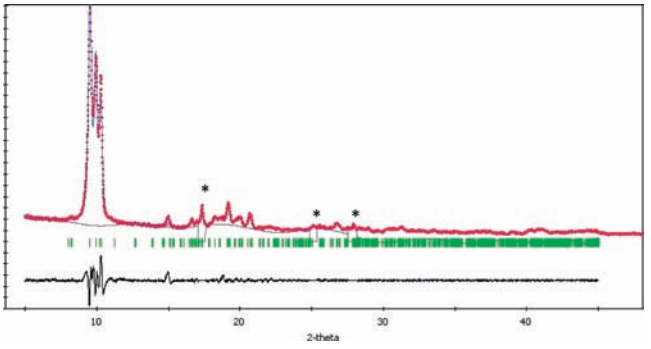

Figure 3. Calculated and experimental diffraction diagrams of compound $\{[Y_6O(OH)_8](NO_3)_2(bdc)(Hbdc)_2\cdot 2NO_3\cdot H_2bdc\}_\infty$. Stars indicate diffraction peaks that correspond to terephthalic acid impurity.

Scanning Electron Microscopy−Energy Dispersive Spectroscopy (SEM-EDS analysis). All SEM observations and EDS measurements were carried out with a Hitachi TM-1000, Tabletop Microscope, version 02.11 (Hitachi High-Technologies, Corporation Tokyo Japan) with an EDS analysis system (SwiftED-TM, Oxford Instruments Link INCA). The detector type is a Silicon drift detector, with an energy resolution of 165 eV, which allows us to detect the element from Na to U. With the software SwiftED-TM, qualitative and quantitative analyses can be realized. All of the samples have been observed by means of an electron beam accelerated at 15 kV, under high vacuum conditions. The samples were assembled on carbon discs, stuck on an aluminum stub fixed at 7 mm from the EDX beam, with an angle of measurement of 22°.

RESULTS AND DISCUSSION

For more than a decade, our group has been involved in the synthesis and the structural characterization of lanthanide-based

Table 3. Selected Bond Distances for $\{[Y_6O(OH)_8](NO_3)_2(bdc)(Hbdc)_2\cdot 2NO_3\cdot H_2bdc\}_\infty$

atom 1	atom 2	symmetry	distances (Å)	atom 1	atom 2	symmetry	distances (Å)
Oc	Y1	$-1+x, y, z$	2.112	O1	Y1	x, y, z	2.145
Oc	Y2	$-1+x, y, z$	2.112	O1	Y2	x, y, z	2.144
Oc	Y3	$-1+x, y, z$	2.118	O1	Y3	$2-x, 1-y, 1-z$	2.254
Y1	O13	$x, -1+y, z$	2.524	O2	Y3	$2-x, 1-y, 1-z$	2.146
Y1	O14	$x, -1+y, z$	2.530	O2	Y2	$2-x, 1-y, 1-z$	2.150
Y2	O11	$2+x, y, 1+z$	2.729	O2	Y1	x, y, z	2.152
Y2	O12	$2+x, y, 1+z$	2.291	O3	Y2	$2-x, 1-y, 1-z$	2.149
Y3	O5	$2+x, -1+y, 1+z$	2.340	O3	Y3	$2-x, 1-y, 1-z$	2.139
Y3	O6	$2+x, -1+y, 1+z$	2.415	O3	Y1	$2-x, 1-y, 1-z$	2.148
O13	C5	x, y, z	1.271	O4	Y1	x, y, z	2.149
O14	C5	x, y, z	1.271	O4	Y2	$2-x, 1-y, 1-z$	2.151
C5	C6	x, y, z	1.398	O4	Y3	x, y, z	2.145
C6	C11	x, y, z	1.403	O11	C4	x, y, z	1.403
C11	C10	x, y, z	1.398	O12	C4	x, y, z	1.402
C10	C9	x, y, z	1.403	C4	C3	x, y, z	1.397
C9	C8	x, y, z	1.403	C3	C1	x, y, z	1.271
C8	C7	x, y, z	1.396	C1	C2	$-1-x, 1-y, -z$	1.402
C7	C6	x, y, z	1.403	C2	C3	x, y, z	1.272
C9	C12	x, y, z	1.397	O6	N1	x, y, z	1.298
C12	O16	x, y, z	1.271	O5	N1	x, y, z	1.299
C12	O15	x, y, z	1.271	N1	O7	x, y, z	1.298

Table 4. Selected Angles for $\{[Y_6O(OH)_8](NO_3)_2(bdc)(Hbdc)_2\cdot 2NO_3\cdot H_2bdc\}_\infty$

atom 1	atom 2	symmetry	atom 3	symmetry	angle (deg)
Y1	$1-x, 1-y, 1-z$	Oc	Y2	$1-x, 1-y, 1-z$	89.82
Y2	$1-x, 1-y, 1-z$	Oc	Y3	$1-x, 1-y, 1-z$	89.50
Y3	$1-x, 1-y, 1-z$	Oc	Y1	$-1+x, y, z$	90.60
Y1	$-1+x, y, z$	Oc	Y2	$-1+x, y, z$	89.82
Y2	$-1+x, y, z$	Oc	Y3	$-1+x, y, z$	89.50

coordination polymers exhibiting potential porosity and/or interesting optical properties.[5,6,56] In the frame of these studies, we have devoted great attention to the 1,4-benzenedicarboxylate (or terephthalate) ligand in association with lanthanide ions.[57−61] Actually, this nontoxic ligand presents a rode-like topology and a structuring character via π-stacking interactions. It also presents a great chemical affinity for rare earth ions. Therefore, when we undertook the present study, we decided to use terephthalate as a probe ligand for evaluating the validity of our approach.

Hydrated hexanuclear complexes easily hydrolyze, even in dry organic solvent, leading to the corresponding hydroxide. We thus decided to use the anhydrous complexes as starting building blocks. The thermal and chemical stabilities of these complexes had previously been studied:[49] these Tb- or Y-containing complexes are thermally stable above 300 °C, and they are readily soluble in dry acetonitrile (3 g L^{-1}).

Considering this background, we have decided to undertake the study of the reaction in acetonitrile between anhydrous hexanuclear complexes and terephthalic acid under solvothermal conditions. Despite great synthetic efforts, it has not been possible to obtain a single crystal suitable for X-ray structure determination. Fortunately, the quality of the XRD diagrams of the microcrystalline powders was good enough to undertake the crystal structure determination.

Crystal Structure of $\{[Y_6O(OH)_8](NO_3)_2(bdc)(Hbdc)_2\cdot 2NO_3\cdot H_2bdc\}_\infty$. The crystal structure has been solved for the Y-containing compound. This crystal structure can be described as the juxtaposition of chains spreading along the $\vec{c}$ direction (see Figure 4). One free molecule of terephthalic acid and two nitrate ions per asymmetric unit lie in the interchains space (see Figure 5).

The hexanuclear entities can be described as quasi-perfect octahedra with one Y(III) ion on each edge and one central oxygen atom (Oc) localized on an inversion center (see Tables 2 and 4). Each face of the octahedron is capped by a μ_3-hydroxyde group. Two out of the six Y(III) atoms (Y2) are bound in a bidentate manner by two bridging terephthalate ions. Two other Y(III) ions (Y1) are bound in a bidentate manner by two monoprotonated terephthalate ions. The protonated carboxylic group spreads in the interchain space. The remaining two Y(III) ions are bound to two bidentate nitrate ions (see Figure 5). Therefore, all six Y(III) ions are seventh coordinated by six oxygen atoms belonging to four capping hydroxide groups, a bidentate ligand (nitrate, terephthalate, or monoprotonated terephthalate) and the central oxygen atom, forming a distorted capped octahedron. This symmetry is in good agreement with what had been encountered in the crystal structure of the anhydrous complex.[25]

Intermetallic distances inside a hexanuclear complex are very short and lay in the range 2.9−4.2 Å (see Table 5).

On the other hand, the hexanuclear entities are rather far from each other (Tables 6 and 7). Actually, the distance between two adjacent hexanuclear entities belonging to the same molecular chain is 12.497 Å, and the shortest distances between hexanuclear entities belonging to adjacent molecular chains are between 10.494 Å and 12.915 Å. Therefore, the Y(III) ions belonging

dx.doi.org/10.1021/ic102036q |*Inorg. Chem.* 2011, 50, 2851–2858

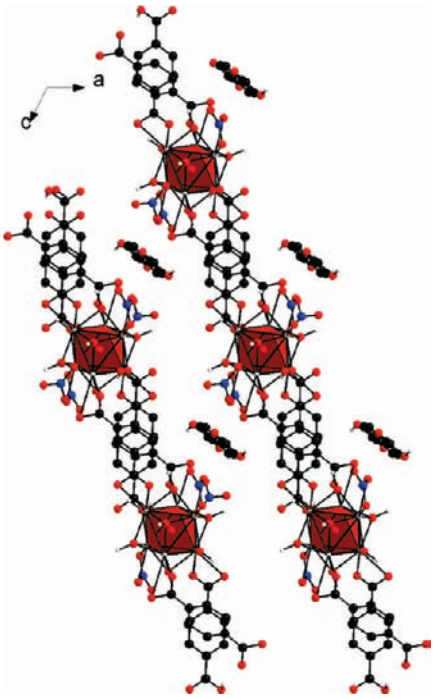

Figure 4. Projection view along the axis of $\{[Y_6O(OH)_8](NO_3)_2(bdc)(Hbdc)_2\cdot 2NO_3\cdot H_2bdc\}_\infty$. The coordination polyhedra of the Y(III) ions are drawn.

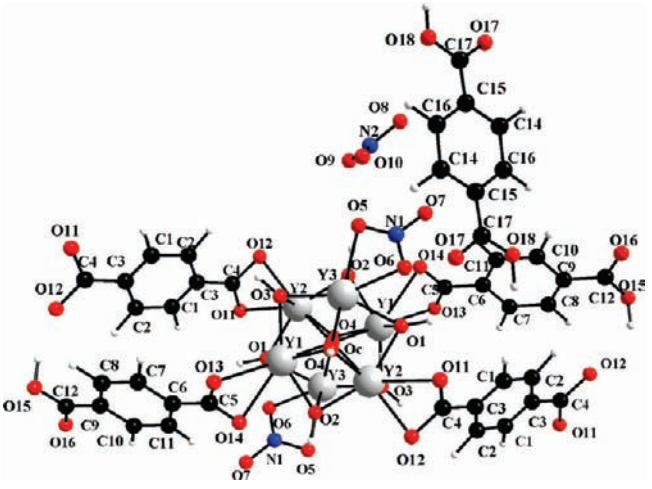

Figure 5. Perspective view of an extended asymmetric unit along with the numbering scheme (hydrogen labels have been omitted for clarity).

to different hexanuclear entities are quite far from each other, that is, between 7.6 Å and 9.9 Å. These quite long distances are promising as far as optical or magnetic properties are concerned.

Thermal Properties of $\{[Y_6O(OH)_8](NO_3)_2(bdc)(Hbdc)_2\cdot 2NO_3\cdot H_2bdc\}_\infty$. The thermal behavior of $\{[Y_6O(OH)_8](NO_3)_2(bdc)(Hbdc)_2\cdot 2NO_3\cdot H_2bdc\}_\infty$ has been studied by TGA/TD and TDXD measurements (see Figure 6).

These experiments both confirm the absence of water or acetonitrile crystallization molecules. They also clearly show that the compound is thermally stable until 200 °C. At last, the TGA is in perfect agreement with the chemical formula obtained from

Table 5. Selected Intermetallic Distances between Y Atoms Belonging to the Same Hexanuclear Entity

atom 1	atom 2	symmetry	distance (Å)
Y1	Y2	x, y, z	2.981
Y1	Y3	x, y, z	2.976
Y1	Y2	$2-x, 1-y, 1-z$	2.992
Y1	Y3	$2-x, 1-y, 1-z$	3.007
Y1	Y1	$2-x, 1-y, 1-z$	4.225
Y2	Y3	$2-x, 1-y, 1-z$	3.005
Y2	Y3	x, y, z	2.975
Y2	Y2	$2-x, 1-y, 1-z$	4.222
Y3	Y3	$2-x, 1-y, 1-z$	4.236

Table 6. Selected Interatomic Distances between Atoms Belonging to Adjacent Hexanuclear Entities

atom 1	atom 2	symmetry	distance (Å)
Oc	Oc	$1+x, y, 1+z$	12.499
Oc	Oc	$-1+x, y, z$	10.496
Oc	Oc	$x, y, 1+z$	12.357
Oc	Oc	$-2+x, y, -1+z$	19.496
Oc	Oc	$x, -1+y, z$	11.530
Oc	Oc	$x, -1+y, 1+z$	16.434
Oc	Oc	$x, -1+y, -1+z$	17.355
Oc	Oc	$1+x, -1+y, z$	12.915<

Table 7. Selected Intermetallic Distances (<10 Å) between Atoms Belonging to Adjacent Hexanuclear Entities

atom 1	atom 2	symmetry	distance (Å)
Y3	Y2	$x, y, -1+z$	9.454
Y2	Y2	$2-x, 1-y, 2-z$	9.636
Y2	Y3	$x, y, 1+z$	9.454
Y2	Y1	$3-x, 1-y, 2-z$	9.533
Y2	Y2	$3-x, 1-y, 2-z$	9.622
Y1	Y2	$3-x, 1-y, 2-z$	9.533
Y1	Y1	$3-x, -y, 1-z$	9.860
Y3	Y1	$x, 1+y, z$	9.639
Y2	Y1	$x, 1+y, z$	9.443
Y1	Y3	$x, -1+y, z$	9.639
Y2	Y3	$2-x, 2-y, 1-z$	8.864
Y2	Y2	$2-x, 2-y, 1-z$	9.144
Y1	Y2	$x, -1+y, z$	9.443
Y3	Y2	$2-x, 2-y, 1-z$	8.864
Y3	Y3	$2-x, 2-y, 1-z$	9.552
Y3	Y2	$3-x, 1-y, 1-z$	8.950
Y1	Y2	$3-x, 1-y, 1-z$	9.621
Y3	Y1	$3-x, 1-y, 1-z$	7.574
Y2	Y1	$-1+x, y, z$	9.813
Y2	Y1	$3-x, 1-y, 1-z$	9.621
Y2	Y3	$-1+x, y, z$	9.151
Y3	Y3	$3-x, 1-y, 1-z$	7.331
Y1	Y3	$3-x, 1-y, 1-z$	7.574
Y2	Y3	$3-x, 1-y, 1-z$	8.950
Y3	Y2	$1+x, y, z$	9.151
Y1	Y2	$1+x, y, z$	9.813
Y1	Y1	$3-x, 1-y, 1-z$	8.872

dx.doi.org/10.1021/ic102036q |*Inorg. Chem.* 2011, 50, 2851–2858

the resolution of the crystal structure and confirms the very low content of impurities in the sample.

Optical Properties of $\{[Tb_6O(OH)_8](NO_3)_2(bdc)(Hbdc)_2\cdot 2NO_3\cdot H_2bdc\}_\infty$. Because the Tb^{3+} ions are well-known for their optical properties,[8,9] the compound $\{[Tb_6O(OH)_8](NO_3)_2(bdc);(Hbdc)_2\cdot 2NO_3\cdot H_2bdc\}_\infty$ has been synthesized. Its isostructurality with the Y-containing compound has been assumed on the basis of elemental analysis and X-ray diffraction diagrams (Figure 7).

These luminescent properties have been studied by fluorimetry. As already observed, the excitation spectra of the compounds present a maximum of intensity at 310 nm.[58] Actually, in this compound, upon excitation of the conjugated organic ligand, intersystem crossing and energy transfer occur, leading to lanthanide ions' luminescence. This phenomenon is well-known and is often referred to as the "antenna effect".[9,62]

$\{[Tb_6O(OH)_8](NO_3)_2(bdc)(Hbdc)_2\cdot 2NO_3\cdot H_2bdc\}_\infty$, under UV irradiation ($\lambda_{exc}$ = 312 nm), exhibits a green luminescence (x = 0.380, y = 0.521, z = 0.099). Its luminescence spectrum recorded at room temperature presents four narrow bands centered at 489, 544, 582, and 618 nm that can be respectively attributed to $^5D_4\rightarrow{}^7F_6$, $^5D_4\rightarrow{}^7F_5$, $^5D_4\rightarrow{}^7F_4$, and $^5D_4\rightarrow{}^7F_3$ transitions (Figure 8).

These luminescent properties are intrinsically not surprising. However, it can be noticed that despite the existence of very short intermetallic distances inside the hexanuclear entities, the luminescence is still fairly strong.

CONCLUSION AND OUTLOOK

In this paper, we have described the synthesis of the first lanthanide-based coordination polymer constructed from a previously isolated hexanuclear complex. This result is very promising and demonstrates the validity of our general strategy for the rational design of new lanthanide-based coordination polymers. Actually, these hexanuclear building blocks offer new perspectives for the design of lanthanide-containing coordination polymers exhibiting original topologies or physical properties. The magnetic and optical properties of these compounds are under study, and the first results are very promising. On the other hand, we are currently trying to obtain a hexanuclear-based 3D coordination polymer exhibiting great porosity.

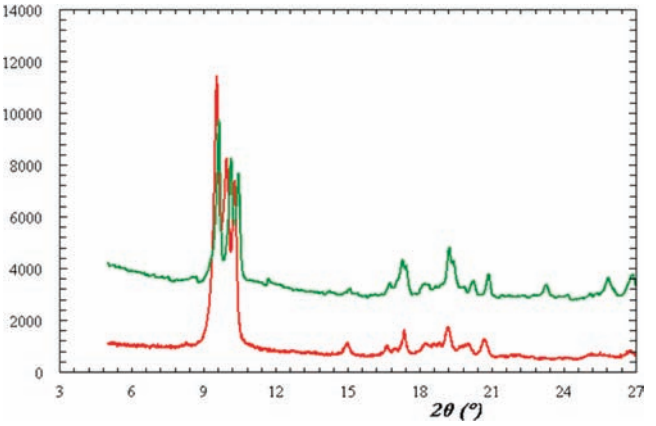

Figure 7. X-ray diffraction diagrams of $\{[Y_6O(OH)_8](NO_3)_2(bdc)(Hbdc)_2\cdot 2NO_3\cdot H_2bdc\}_\infty$ (down) and of $\{[Tb_6O(OH)_8](NO_3)_2(bdc)(Hbdc)_2\cdot 2NO_3\cdot H_2bdc\}_\infty$ (up).

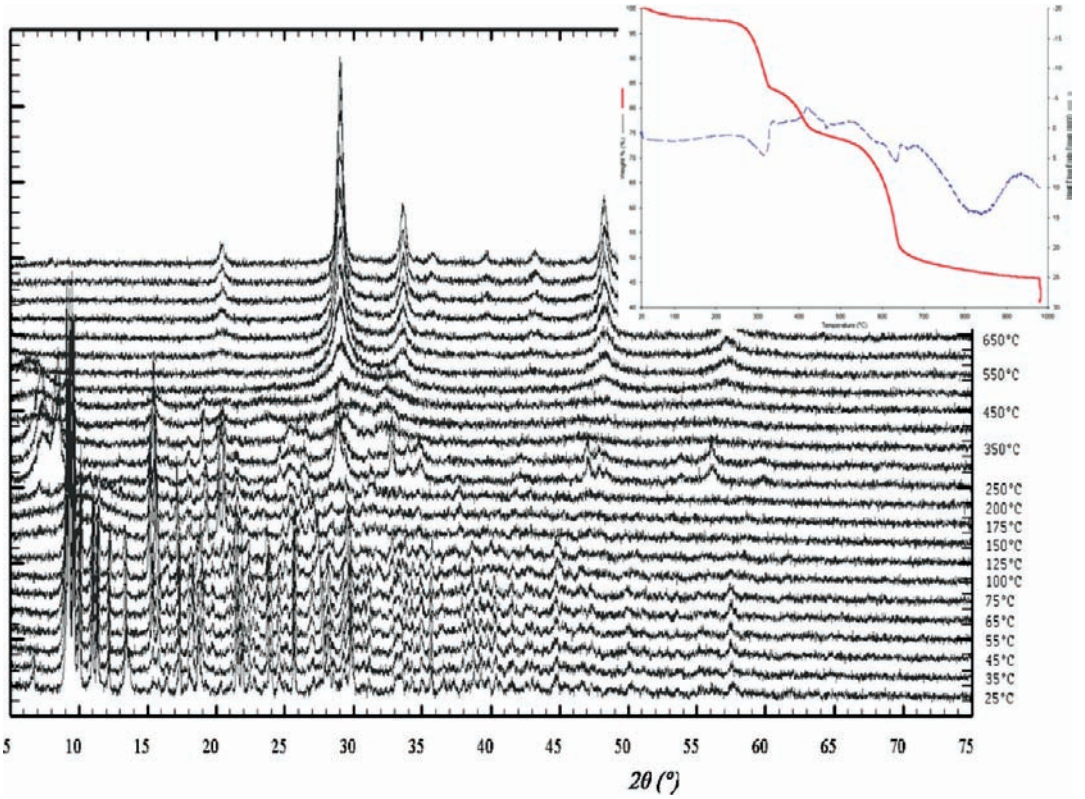

Figure 6. TDXD measurements between room T and 1000 °C of $\{[Y_6O(OH)_8](NO_3)_2(bdc)(Hbdc)_2\cdot 2NO_3\cdot H_2bdc\}_\infty$. Inset, the TGA/TD.

dx.doi.org/10.1021/ic102036q |*Inorg. Chem.* 2011, 50, 2851–2858

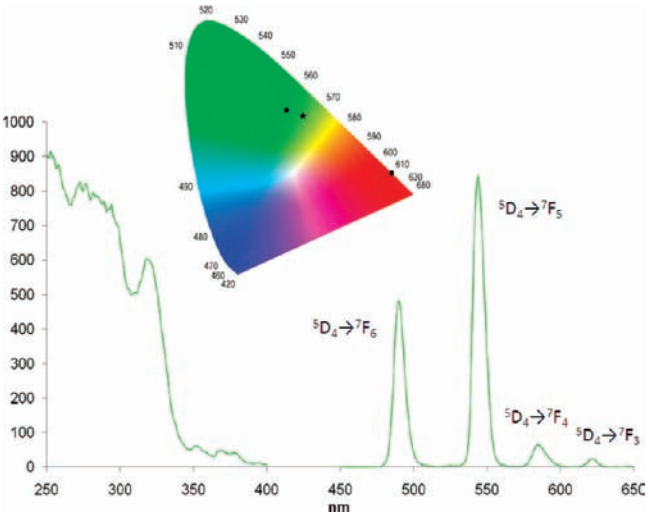

Figure 8. Excitation (λ_{em} = 545 nm) and luminescence (λ_{exc} = 312 nm) spectra of $\{[Tb_6O(OH)_8](NO_3)_2(bdc)(Hbdc)_2 \cdot 2NO_3 \cdot H_2bdc\}_\infty$. Inset, the colorimetric coordinates of the compound in a chromaticity diagram. The colorimetric coordinates of the references are symbolized by ●, the ones of the compound $\{[Tb_6O(OH)_8](NO_3)_2(bdc)(Hbdc)_2 \cdot 2NO_3 \cdot H_2bdc\}_\infty$ by ★.

■ ASSOCIATED CONTENT

Supporting Information. A crystallographic information file (CIF) is provided. This material is available free of charge via the Internet at http://pubs.acs.org.

■ AUTHOR INFORMATION

Corresponding Author
*E-mail: Olivier.guillou@insa-rennes.fr.

■ REFERENCES

(1) Guillou, O.; Daiguebonne, C. In *Handbook on the Physics and Chemistry of Rare Eaths*; Gschneider, K. A.; Bünzli, J. C. G.; Pecharsky, V. K., Eds.; Elsevier: Amsterdam, 2005; vol 34, pp 359−404.
(2) Serpaggi, F.; Férey, G. *Microporous Mesoporous Mater.* **1999**, *32*, 311–318.
(3) Devic, T.; Serre, C.; Audebrand, N.; Marrot, J.; Férey, G. *J. Am. Chem. Soc.* **2005**, *127*, 12788–12789.
(4) Kerbellec, N.; Daiguebonne, C.; Bernot, K.; Guillou, O.; Le Guillou, X. *J. Alloys Compd.* **2008**, *451*, 377–383.
(5) Qiu, Y.; Deng, H.; Yang, S.; Mou, J.; Daiguebonne, C.; Kerbellec, N.; Guillou, O.; Batten, S. R. *Inorg. Chem.* **2009**, *48*, 3976–3981.
(6) Kustaryono, D.; Kerbellec, N.; Calvez, G.; Daiguebonne, C.; Guillou, O. *Cryst. Growth Des.* **2010**, *10*, 775–781.
(7) Binnemans, K. *Chem. Rev.* **2009**, *109*, 4283–4374.
(8) Bünzli, J. C. G.; Piguet, C. *Chem. Soc. Rev.* **2005**, *34*, 1048–1077.
(9) Bünzli, J. C. G. *Acc. Chem. Res.* **2006**, *39*, 53–61.
(10) Eliseeva, S. V.; Bünzli, J. C. G. *Chem. Soc. Rev.* **2010**, *39*, 189–227.
(11) Tremblay, M. S.; Halim, M.; Sames, D. *J. Am. Chem. Soc.* **2007**, *129*, 7570–7577.
(12) Samuel, A. P. S.; Xu, J.; Raymond, K. N. *Inorg. Chem.* **2009**, *48*, 687–698.
(13) Eddaoudi, M.; Kim, J.; Rosi, N.; Vodak, D.; Wachter, J.; O'Keeffe, M.; Yaghi, O. M. *Science* **2002**, *295*, 469–472.
(14) Deng, H.; Doonan, C. J.; Furukawa, H.; Ferreira, R. B.; Towne, J.; Knobler, C. B.; Wang, B.; Yaghi, O. M. *Science* **2010**, *327*, 846–850.
(15) Ma, B. Q.; Zhang, D. S.; Gao, S.; Jin, T. Z.; Yan, C. H.; Xu, G. X. *Angew. Chem., Int. Ed.* **2000**, *39*, 3644–3646.
(16) Wang, R.; Liu, H.; Carducci, M. D.; Jin, T.; Zheng, C.; Zheng, Z. *Inorg. Chem.* **2001**, *40*, 2743–2750.
(17) Zheng, X. J.; Jin, L. P.; Gao, S. *Inorg. Chem.* **2004**, *43*, 1600–1602.
(18) Jia, D. X.; Zhang, Y.; Dai, J.; Zhu, Q. Y.; Lu, W.; Guo, W. J. *Inorg. Chem. Commun.* **2005**, *8*, 588–591.
(19) Weng, D.; Zheng, X.; Jin, L. *Eur. J. Inorg. Chem.* **2006**, 4184–4190.
(20) Park, Y. K.; Choi, S. B.; Kim, H.; Won, B.-H.; Choi, K.; Choi, J. S.; Ahn, W. S.; Won, N. *Angew. Chem., Int. Ed.* **2007**, *46*, 8230–8233.
(21) Ma, S.; Yuan, D.; Wang, X. S.; Zhou, H. C. *Inorg. Chem.* **2009**, *48*, 2072–2077.
(22) Shi, F. N.; Cunha-Silva, L.; Trindade, T.; Paz, F. A. A.; Rocha, J. *Cryst. Growth Des.* **2009**, *9*, 2098–2109.
(23) Liu, J.; Meyers, E. A.; Shore, S. G. *Inorg. Chem.* **1998**, *37*, 5410–5411.
(24) Mahé, N.; Guillou, O.; Daiguebonne, C.; Gérault, Y.; Caneschi, A.; Sangregorio, C.; Chane-Ching, J. Y.; Car, P. E.; Roisnel, T. *Inorg. Chem.* **2005**, *44*, 7743–7750.
(25) Calvez, G.; Daiguebonne, C.; Guillou, O.; Le Dret, F. *Eur. J. Inorg. Chem.* **2009**, 3172–3178.
(26) Fenske, D.; Zhu, N.; Langetepe, T. *Angew. Chem., Int. Ed.* **1998**, *37*, 2640–2644.
(27) Müller, A.; Krickemeyer, E.; Bögge, H.; Schmidtmann, M.; Peters, F. *Angew. Chem., Int. Ed.* **1998**, *37*, 3360–3363.
(28) Wang, R.; Zheng, Z.; Jin, T.; Staples, R. J. *Angew. Chem., Int. Ed.* **1999**, *38*, 1813–1815.
(29) Wang, R.; Carducci, M. D.; Zheng, Z. *Inorg. Chem.* **2000**, *39*, 1836–1837.
(30) Zheng, Z.; Wang, R. *Comments Inorg. Chem.* **2000**, *22*, 1–30.
(31) Wang, R.; Selby, H. D.; Liu, H.; Carducci, M. D.; Jin, T.; Zheng, Z.; Anthis, J. W.; Staples, R. J. *Inorg. Chem.* **2002**, *41*, 278–286.
(32) Zheng, Z. *Chemtracts Inorg. Chem.* **2003**, *16*, 1–12.
(33) Wang, R.; Song, D.; Wang, S. *Chem. Commun.* **2002**, 368–369.
(34) Xu, G.; Wang, Z. M.; He, Z.; Lu, Z.; Liao, C. S.; Yan, C. H. *Inorg. Chem.* **2002**, *41*, 6802–6807.
(35) Ma, B. Q.; Zhang, D. S.; Gao, S.; Jin, T. Z.; Yan, C. H. *New J. Chem.* **2000**, *24*, 251–252.
(36) Anwander, R.; Munck, F. C.; Priermeier, T.; Scherer, W.; Runte, O.; Hermann, W. A. *Inorg. Chem.* **1997**, *36*, 3545–3552.
(37) Hubert-Pfalzgraf, L. G.; Miele-Pajot, N.; Papiernik, R.; Vaissermann, J. *J. Chem. Soc., Dalton Trans.* **1999**, 4127–4130.
(38) Rossmanith, K.; Unfried, P. *Monatsh. Chem.* **1989**, *120*, 849–862.
(39) Unfried, P.; Rossmanith, K.; Blaha, H. *Monatsh. Chem.* **1991**, *122*, 635–644.
(40) Unfried, P.; Rossmanith, K. *Monatsh. Chem.* **1992**, *123*, 1–8.
(41) Lengauer, C. L.; Giester, G.; Unfried, P. *Powder Diffraction* **1994**, *9*, 115–118.
(42) Zak, Z.; Unfried, P.; Giester, G. *J. Alloys Compd.* **1994**, *205*, 235–242.
(43) Giester, G.; Unfried, P.; Zak, Z. *J. Alloys Compd.* **1997**, *257*, 175–181.
(44) Unfried, P. *Thermochim. Acta* **1997**, *303*, 119–127.
(45) Giester, G.; Zak, Z.; Unfried, P. *J. Alloys Compd.* **2009**, *481*, 116–128.
(46) Pelloquin, D.; Louër, D.; Louër, M. *J. Solid State Chem.* **1994**, *112*, 182–188.
(47) Beal, G. W.; Milligan, W. O.; Dillin, D. R.; Williams, R. J.; Mc Coy, J. J. *Acta Crystallogr., Sect. B* **1976**, *32*, 2227–2229.
(48) Calvez, G.; Guillou, O.; Daiguebonne, C.; Car, P.-E.; Guillerm, V.; Gérault, Y.; Dret, F. L.; Mahé, N. *Inorg. Chim. Acta* **2008**, *361*, 2349–2356.
(49) Calvez, G.; Daiguebonne, C.; Guillou, O.; Pott, T.; Méléard, P.; Le Dret, F. *C. R. Acad. Sci. Paris* **2010**, *13*, 715–730.

(50) Guillou, O.; Daiguebonne, C.; Calvez, G.; Le Dret, F.; Car, P. E. *J. Alloys Compd.* **2008**, *451*, 329–333.
(51) Calvez, G.; Bernot, K.; Guillou, O.; Daiguebonne, C.; Caneschi, A.; Mahé, N. *Inorg. Chim. Acta* **2008**, *361*, 3997–4003.
(52) *Accelrys*; Accelrys Software Inc.: San Diego, CA, 2005.
(53) Smith, G. S.; Snyder, R. L. *J. Appl. Crystallogr.* **1979**, *12*, 60–65.
(54) Young, R. A. *The Rietveld Method*; Oxford University Press: Oxford, England, 1993.
(55) Wyszecki, G. In *Handbook of Optics*; Driscoll, W. G., Vaughan, W., Eds.; MacGraw-Hill Book Company: New York, 1978; pp 1−15.
(56) Luo, Y.; Calvez, G.; Freslon, S.; Daiguebonne, C.; Roisnel, T.; Guillou, O. *Inorg. Chim. Acta* **2011**, *368*, 170–178.
(57) Daiguebonne, C.; Kerbellec, N.; Bernot, K.; Gérault, Y.; Deluzet, A.; Guillou, O. *Inorg. Chem.* **2006**, *45*, 5399–5406.
(58) Daiguebonne, C.; Kerbellec, N.; Guillou, O.; Bünzli, J. C. G.; Gumy, F.; Catala, L.; Mallah, T.; Audebrand, N.; Gérault, Y.; Bernot, K.; Calvez, G. *Inorg. Chem.* **2008**, *47*, 3700–3708.
(59) Kerbellec, N.; Catala, L.; Daiguebonne, C.; Gloter, A.; Stephan, O.; Bünzli, J. C. G.; Guillou, O.; Mallah, T. *New J. Chem.* **2008**, *32*, 584–587.
(60) Kerbellec, N.; Kustaryono, D.; Haquin, V.; Etienne, M.; Daiguebonne, C.; Guillou, O. *Inorg. Chem.* **2009**, *48*, 2837–2843.
(61) Haquin, V.; Gumy, F.; Daiguebonne, C.; Bünzli, J. C. G.; Guillou, O. *Eur. J. Inorg. Chem.* **2009**, 491–497.
(62) Pellé, F.; Surblé, S.; Serre, C.; Millange, F.; Férey, G. *J. Lumin.* **2007**, *122−123*, 492–495.